Proc. Asia-Pacific Conf. on Semiconducting Silicides and Related Materials 2016
JJAP Conf. Proc. **5**, 011501 (2017) https://doi.org/10.7567/JJAPCP.5.011501

Temperature-dependent Magnetoresistance Effects in $Fe_3Si/FeSi_2/Fe_3Si$ Trilayered Spin Valve Junctions

Kazuya Ishibashi[1], Kazuki Kudo[1], Kazutoshi Nakashima[1], Yuki Asai[1], Ken-ichiro Sakai[2]*, Hiroyuki Deguchi[3], and Tsuyoshi Yoshitake[1]**

[1] *Department of Applied Science for Electronics and Materials, Kyushu University, Kasuga, Fukuoka 816-8580, Japan*
[2] *Department of Control and Information Systems Engineering, National Institute of Technology, Kurume College, Kurume, Fukuoka 830-8555, Japan*
[3] *Department of Basic Sciences, Faculty of Engineering, Kyushu Institute of Technology, Kitakyushu, Fukuoka 804-8550, Japan*

E-mail: *kenichiro_sakai@kyudai.jp; **tsuyoshi_yoshitake@kyudai.jp

(Received October 1, 2016)

$Fe_3Si/FeSi_2/Fe_3Si$ trilayered junctions were fabricated by facing targets direct-current sputtering combined with a mask method, and the spin valve signals of the junctions were studied in the temperature range from 50 to 300 K. Whereas the magnetoresistance ratio of giant magnetoresistance and tunnel magnetoresistance junctions monotonically increases with decreasing temperature, that of our samples has the maximum value around 80 K and decreases with decreasing temperature at lower than 80 K, which might be due to an increase in the electrical conductivity mismatch between the metallic Fe_3Si layers and semiconducting $FeSi_2$ interlayer in the low temperature range .

1. Introduction

Research on spin-based electronics (spintronics) that utilizes not only the electric charge of carriers but also their spin has actively been progressed since the discovery of giant magnetoresistance (GMR) [1,2] and tunnel magnetoresistance (TMR) [3,4] effects. These phenomena have already been applied to magnetic heads and magnetic random access memories (MRAM).

Heterostructural junctions comprising ferromagnetic and semiconducting layers such as GaMnAs/GaAs [5], GaMnAs/AlAs [6,7], Fe/Si [8,9,10], and $Fe/Fe_{1-x}Si_x$ [11,12] has received attention from physical and practical viewpoints, since the electric state of semiconductors is changeable by irradiating and heating (cooling), resulting in a change in the magnetoresistance (MR) effect.

The Fe-Si system has various phases such as semiconducting β-$FeSi_2$, amorphous and nanocrystalline $FeSi_2$, nonmagnetic metallic FeSi, and ferromagnetic Fe_3Si. Recently, Fe_3Si has been employed as a spin injection electrode in Co60Fe40/AlOx/Fe_3Si tunnel junctions [13] and in spin injection to Si [14]. We have studied spintronics based on a Fe-Si system comprising ferromagnetic Fe_3Si and semiconducting $FeSi_2$ thus far [15,16,17,18,19,20,21,22,23,24,25,26]. The combination of Fe_3Si and $FeSi_2$ has the following merits [15,16,17,27,28]: (i) the spin injection efficiency might be higher than that in TMR junctions, because the mismatch of the electrical conductivities is less than an order of magnitude, and d electrons contribute to electrical conduction in both layers, (ii) Fe_3Si can be epitaxially grown on Si(111) substrates even at room substrate temperature, which is beneficial to the coherent transportation of spin-polarized electrons, and (iii) Fe_3Si is feasible for a practical use since it has a high Curie temperature of 840 K and a large saturation magnetization which is half of that of Fe. Additionally, $FeSi_2$ has a large optical absorption coefficient, which is two

orders of magnitude larger than that of Si at 1.2 eV.

The MR ratio is an important factor for spin valve junctions, and the value is dependent on temperature. For example, Sakuraba *et al.* reported the TMR ratio of Co_2MnSi/Al-O/Co_2MnSi magnetic tunnel junctions dramatically increases with decreasing temperature from 67 % at 300 K to 570 % at 2 K [29]. The origin of the temperature-dependent TMR ratio has been discussed as (i) an increase in the tunneling conductance for an antiparallel alignment due to spin-flip scattering by thermally excited magnons [30] and (ii) a reduction in the exchange energy of Co at interfaces with barriers [31]. For GMR junctions, the GMR ratio monotonically increases with decreasing temperature [32,33]. There have been few reports on the temperature dependence of the MR ratio for spin valves comprising ferromagnetic and semiconducting layers thus far.

The electrical injection of spin-polarized carriers into semiconductors has received much attention from the viewpoints of physics and application to spintronics devices, and has actively been studied theoretically and experimentally. It is well known that a huge electrical conductivity mismatch between ferromagnetic metallic and semiconducting layers makes the spin injection efficiency drop off rapidly [34]. To overcome this problem, the formation of Schottky barriers at interfaces and the physical insertion of discrete insulating layer between ferromagnetic and semiconducting layers have been proposed [35,36]. On the other hand, uniquely, a specific to our spin valves is that the mismatch of the electrical conductivities between ferromagnetic Fe_3Si and semiconducting $FeSi_2$ is less than an order of magnitude.

In this research, the temperature dependence of the MR ratio for $Fe_3Si/FeSi_2/Fe_3Si$ trilayered spin valve junctions was experimentally studied. We report that the MR ratio decreases with decreasing temperature at lower than 80 K, which is distinctively different from those of GMR and TMR junctions and which might be attributable to enlarged conductivity mismatch between ferromagnetic metallic Fe_3Si and semiconducting $FeSi_2$ layers at the low temperature.

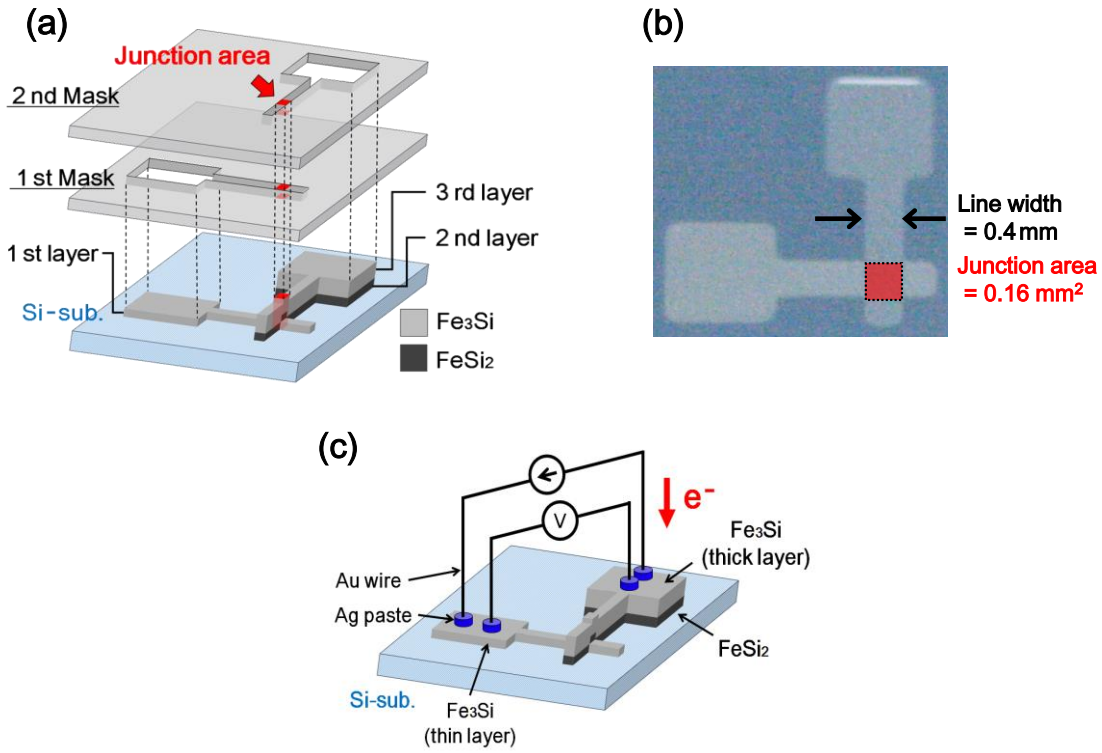

Fig. 1. (a) Schematic diagram of deposition procedure of $Fe_3Si/FeSi_2/Fe_3Si$ junction, (b) top view of the junction, and (c) electrical circuit for measuring electrical resistance of the junction.

2. Experimental methods

Fe_3Si (700 nm)/$FeSi_2$ (10 nm)/Fe_3Si (100 nm) trilayered films were deposited by facing targets direct-current sputtering (FTDCS) combined with a mask method, as shown in Fig. 1(a). First, a p-type Si(111) substrate with specific resistance range of 1000-3000 Ω·cm, which was produced by the floating zone (FZ) method, was cleaned with 1% hydrofluoric acid and rinsed in deionized water before it was set into a chamber of FTDCS apparatus. The bottom Fe_3Si layer (100 nm) was deposited on the Si (111) substrate, using the 1st mask with a line width of 0.4 mm. After that, the samples were temporarily taken out from the apparatus for the replacement of the mask. And the $FeSi_2$ (10 nm) interlayer and top Fe_3Si (700 nm) layers were successively deposited with 2nd mask. A resultant junction area is 0.16 mm^2. All depositions were performed at a substrate temperature of 300 °C. The base pressure was lower than 3×10^{-5} Pa and the film deposition was carried out at constant pressure of 1.33×10^{-1} Pa.

After the deposition, the crystalline structures of the junctions were characterized by X-ray diffraction (XRD) using Cu Kα radiation. The magnetization curves were measured by a vibrating sample magnetometer (VSM) at room temperature, and the external magnetic field was applied in-plane and parallel to the long side of the bottom Fe_3Si layers. It corresponds to the horizontal direction in Fig. 1(b). To investigate the temperature dependence of spin valve effects in the junctions, the magnetization and MR curves of the junctions were measured by a superconducting quantum interference device (SQUID) in the temperature range from 300 down to 5 K. In the MR curve measurement, as shown in Fig. 1(c), the electrical resistance was calculated from the voltage between the top and bottom Fe_3Si layers measured under a fixed current of 10 mA.

3. Results and discussion

Figures 2(a) and 2(b) show XRD patterns measured in 2θ with an incidence angle of 1.5 ° and in 2θ-θ, respectively. The 2θ-θ pattern exhibits Fe_3Si-220 and 222 peaks, and the 2θ pattern exhibits Fe_3Si-220 and 400 peaks. Here, the index for Fe_3Si was based on DO_3-Fe_3Si lattices. The Fe_3Si-220 peak is attributable to non-oriented crystallites. The inset of Fig. 2(b) shows a pole-figure concerning the

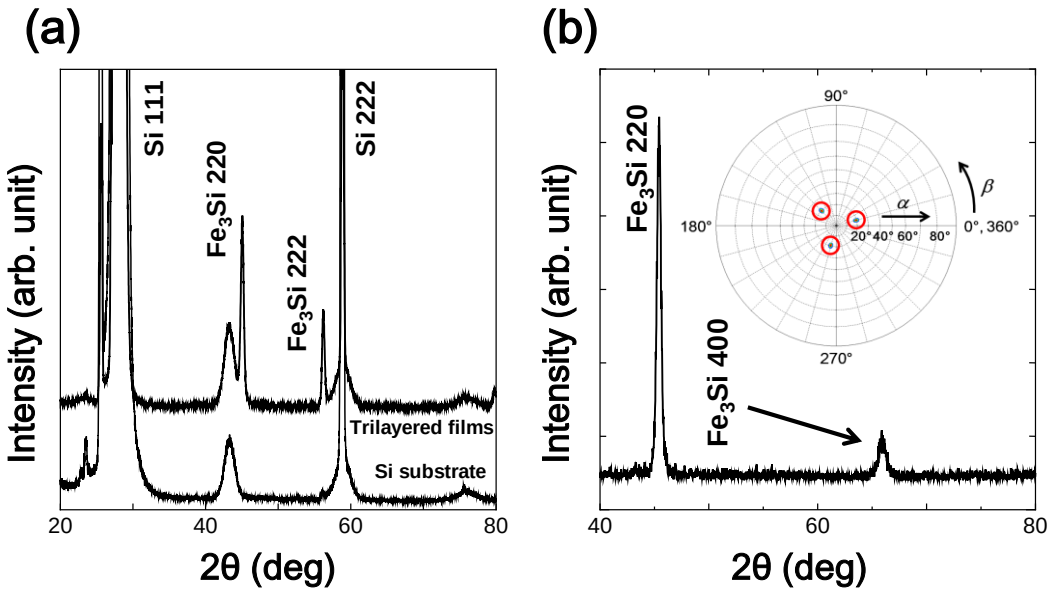

Fig. 2. XRD patterns of $Fe_3Si/FeSi_2/Fe_3Si$ junction, measured in (a) 2θ-θ and (b) 2θ. Inset shows pole figure concerning Fe_3Si-422 planes.

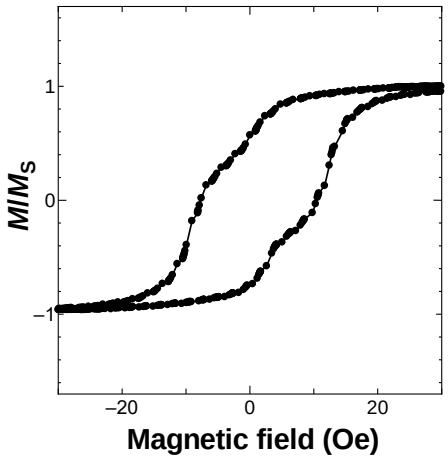

Fig. 3. Typical magnetization curve of $Fe_3Si/FeSi_2/Fe_3Si$ junction, measured at room temperature.

Fe_3Si-422 plane with a rotation axis of Fe_3Si[222]. It was confirmed that oriented crystallites are also in-plane ordered. In our previous study, we confirmed that B2-type Fe_3Si layers are epitaxially grown from the first layer on Si(111) up to the top layer across the $FeSi_2$ layer with the same orientation relationship as the first layer for structurally similar films, by transmission electron microscopy [16]. Totally considering the results including those of our previous research, wherein Fe_3Si thin films are epitaxially grown on Si(111) substrate even at room temperature [16], the bottom Fe_3Si layer should epitaxially be grown on the Si(111) substrate. On the other hand, although the top Fe_3Si thick layer deposited on $FeSi_2$ layer might partially be oriented with the same orientation relationship as the bottom layer, it might be predominantly polycrystalline due to the temporal exposure to air for the replacement of the masks.

A typical magnetization curve of the junction is shown in Fig. 3. The shape of the magnetization curve has clear steps that evidently indicate the formation of antiparallel alignment of magnetizations owing to the difference in the coercive force between the top and bottom Fe_3Si layers, which was similarly observed at low temperatures. The soft ferromagnetic layers should be the bottom Fe_3Si layer epitaxially grown on Si(111) from the previous study [19,22,25]. The top Fe_3Si layer comprising polycrystalline grains and oriented grains with the same orientation relationship with the epitaxial Fe_3Si grains in the bottom layer probably has the larger coercive force. In addition, note that a large difference in the thickness between the top and bottom layers might facilitate the generation of the coercive force difference.

The MR curves of the junction were measured at different temperatures. Figure 4(a) and 4(b) show the survey plots of the MR curves in serial resistance and the temperature dependence of the serial resistance under the parallel alignment of magnetizations (at 8 Oe). The MR curves weakly exhibit spin valve signals around zero magnetic field. The serial resistance decreases with decreasing temperature, which indicates that an increase in the electrical resistivity of the $FeSi_2$ layer with decreasing temperature is negligibly small as compared with a decrease in the electrical resistivity of both Fe_3Si layers, since the thickness (10 nm) of the $FeSi_2$ layer is much smaller than the total thickness (800 nm) of the top and bottom Fe_3Si layers.

However, as shown in Fig. 4(b), the change of the serial resistance for temperature is not proportional in the temperature range of lower than 80 K, which implies the electrical contribution of the semiconducting $FeSi_2$ layer. Figure 5 shows the temperature dependence of the electrical resistivity of a 100 nm $FeSi_2$ monolayer film deposited on a quartz substrate by FTDCS. The deposition was carried out at the same preparation conditions as that of the $FeSi_2$ layer of the junction. The electrical resistivity increases with decreasing temperature, which is a semiconducting behavior.

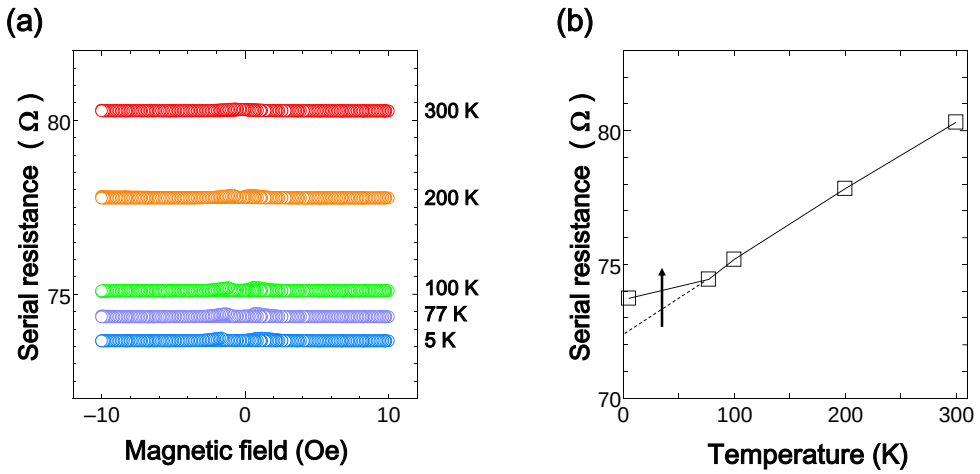

Fig. 4. (a) Survey MR curves of $Fe_3Si/FeSi_2/Fe_3Si$ junction, measured at temperatures of 300, 200, 100, 77, and 5 K. (b) Temperature dependence of junction serial resistance.

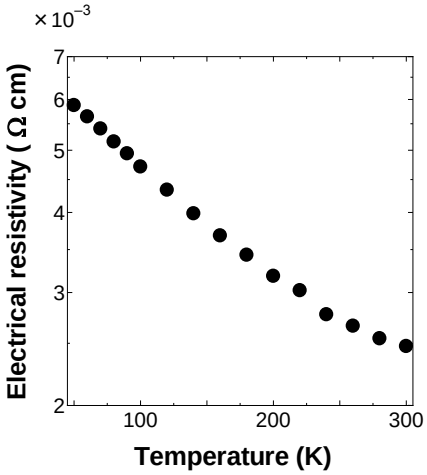

Fig. 5. Change in electrical resistivity of 100 nm $FeSi_2$ monolayer film deposited on quartz substrate at the same preparation conditions as that of $FeSi_2$ layer of $Fe_3Si/FeSi_2/Fe_3Si$ junction by FTDCS.

Although totally-800-nm-thickness Fe_3Si layers predominantly determine the serial resistance of the junction, an increase in the electrical resistance of the 10 nm $FeSi_2$ layer should affect the junction serial resistance at the low temperatures of less than 80 K.

The MR curves shown in Fig. 4(a) are plotted in MR ratio in Fig. 6. All MR curves at the different temperatures clearly exhibit spin valve signals induced by a change in the magnetization alignment. Generally, the MR ratio monotonically increases with decreasing temperature or saturates at low temperatures due to the suppression of electron-phonon scattering [37]. On the other hand, in our study, the MR ratio has the maximum around 80 K, as shown in Fig. 7, which is distinctively different from the temperature dependence in the MR ratio of GMR and TMR junctions.

As a reason for the decrease in the MR ratio at temperatures of lower than 80 K, we consider an enlarged mismatch in the electrical conductivity between the ferromagnetic metallic Fe_3Si and semiconducting $FeSi_2$ layers. For GMR junctions comprising only metallic layers, the conductivity mismatch between ferromagnetic and nonmagnetic layers hardly changes, because the electrical conductivity of all layers monotonically decreases with decreasing temperature. On the other hand,

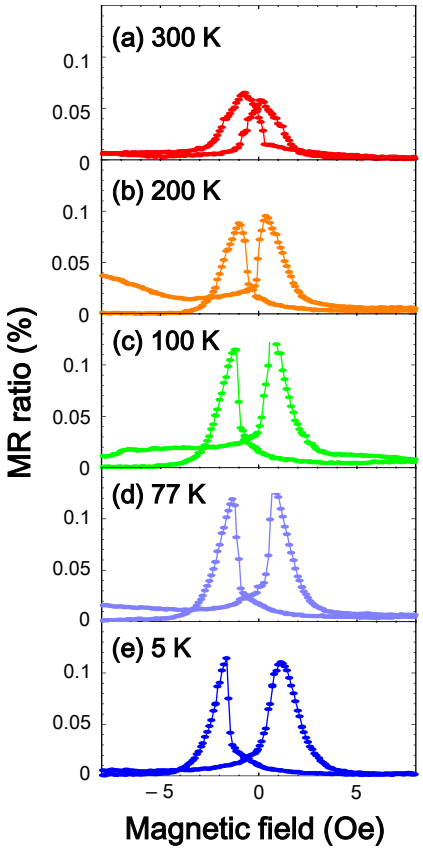

Fig. 6. MR curves of $Fe_3Si/FeSi_2/Fe_3Si$ junction, measured at 300, 200, 100, 77, and 5 K.

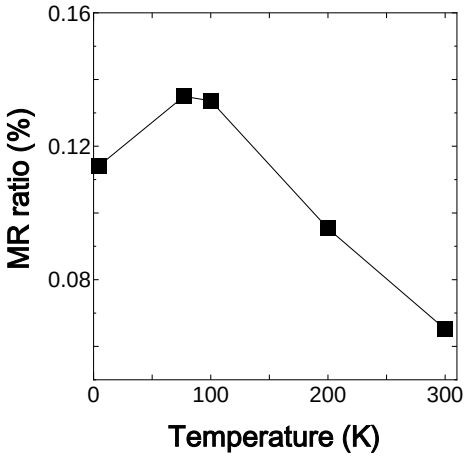

Fig. 7. Change in MR ratio with temperature.

for the junctions comprising the metallic Fe_3Si and semiconducting $FeSi_2$ layers in our study, the Fe_3Si and $FeSi_2$ layers show opposite temperature-dependences in the electrical resistivity. Owing to their behaviors, the conductivity mismatch gradually increases with decreasing temperature. At the low temperatures of lower than 80 K, the enlarged mismatch should degrade the injection of spin-polarized carriers, which might result in the decrease in the MR ratio.

4. Conclusion

$Fe_3Si/FeSi_2/Fe_3Si$ trilayered junctions were prepared by FTDCS, and the temperature-dependent spin valve behaviors of the junctions were studied experimentally. The MR ratio has a maximum around 80 K and decreases with decreasing temperature at temperatures of lower than 80 K. This might be because of the degraded injection of spin polarized carriers, which is probably caused by enlarged conductivity mismatches between the metallic Fe_3Si and semiconducting $FeSi_2$ layers at the low temperatures.

Acknowledgment

This work was supported by JSPS KAKENHI Grant Number 15K21594 and Yoshida Grant from Yoshida Academic Education Promotion Association. The VSM and SQUID measurements were performed at Fukuoka Institute of Technology and Kyushu Institute of Technology, respectively.

References

[1] G. Binasch, P. Grünberg, F. Saurenbach, and W. Zinn, Phys. Rev. B **39**, 4828 (1989).
[2] M. N. Baibich, J. M. Broto, A. Fert, F. Nguyen Van Dau, F. Petroff, P. Etienne, G. Creuzet, A. Friederich, and J. Chazelas, Phys. Rev. Lett. **61**, 2472 (1988).
[3] M. Julliere, Phys. Lett. A **54**, 225 (1975).
[4] T. Miyazaki and N. Tezuka, J. Magn. Magn. Mater. **139**, L231 (1995).
[5] D. Chiba, Y. Sato, T. Kita, F. Matsukura, and H. Ohno, Phys. Rev. Lett. **93**, 216602 (2004).
[6] R. Moriya, K. Hamaya, A. Oiwa, and H. Munekata, Jpn. J. Appl. Phys. **43**, L825 (2004).
[7] M. Watanabe, J. Okabayashi, H. Toyao, T. Yamaguchi, and J. Yoshino, Appl. Phys. Lett. **92**, 082506 (2008).
[8] K. Inomata, K. Yusu, and Y. Saito, Phys. Rev. Lett. **74**, 1863 (1995).
[9] Eric E. Fullerton, J. E. Mattson, S. R. Lee, C. H. Sowers, Y. Y. Huang, G. Felcher, and S. D. Bader, J. Appl. Phys. **73**, 6335 (1993).
[10] Eric E. Fullerton, J. E. Mattson, S. R. Lee, C. H. Sowers, Y. Y. Huang, G. Felcher, and S. D. Bader, J. Magn. Magn. Mater. **117**, L301 (1992).
[11] J. E. Mattson, Sudha Kumar, Eric E. Fullerton, S. R. Lee, C. H. Sowers, M. Grimsditch, and S. D. Bader, Phys. Rev. Lett. **71**, 185 (1993).
[12] Y. Endo, O. Kitakami, and Y. Shimada, Phys. Rev. B **59**, 4279 (1999).
[13] Y. Fujita, S. Yamada, G. Takemoto, S. Oki, Y. Maeda, M. Miyao, and K. Hamaya, Jpn. J. Appl. Phys. **52**, 04CM02 (2013).
[14] K. Hamaya, Y. Ando, T. Sadoh, and M. Miyao, Jpn. J. Appl. Phys. **50**, 010101 (2011).
[15] T. Yoshitake, T. Ogawa, D. Nakagauchi, D. Hara, M. Itakura, N. Kuwano, and Y. Tomokiyo, Appl. Phys. Lett. **89**, 253110 (2006).
[16] K. Takeda, T. Yoshitake, D. Nakagauchi, T. Ogawa, D. Hara, M. Itakura, N. Kuwano, Y. Tomokiyo, T. Kajiwara, and K. Nagayama, Jpn. J. Appl. Phys. **46**, 7846 (2007).
[17] K. Takeda, T. Yoshitake, Y. Sakamoto, T. Ogawa, D. Hara, M. Itakura, N. Kuwano, T. Kajiwara, and K. Nagayama, Appl. Phys. Express **1**, 021302 (2008).
[18] S. Hirakawa, T. Sonoda, K. Sakai, K. Takeda, and T. Yoshitake, Jpn. J. Appl. Phys. **50**, 08JD06 (2011).
[19] K. Sakai, T. Sonoda, S. Hirakawa, K. Takeda, and T. Yoshitake, Jpn. J. Appl. Phys. **51**, 028004 (2012).
[20] K. Sakai, Y. Noda, K. Takeda, M. Takeda, and T. Yoshitake, Phys. Status Solidi C **10**, 1862 (2013).
[21] K. Sakai, Y. Noda, D. Tsumagari, H. Deguchi, K. Takeda, and T. Yoshitake, Phys. Status Solidi A **211**, 323 (2014).
[22] K. Sakai, Y. Noda, T. Daio, D. Tsumagari, A. Tominaga, K. Takeda, and T. Yoshitake, Jpn. J. Appl. Phys. **53**, 02BC15 (2014).
[23] K. Sakai, Y. Asai, M. Takeda, K. Ishibashi, Y. Noda, K. Takeda, and T. Yoshitake, JJAP Conf. Proc. **3**, 011502 (2015).
[24] K. Sakai, Y. Asai, Y. Noda, T. Daio, A. Tominaga, K. Takeda, and T. Yoshitake, JJAP Conf. Proc. **3**,

011503 (2015).
[25] Y. Asai, K. Sakai, K. Ishibashi, K. Takeda, and T. Yoshitake, JJAP Conf. Proc. **3**, 011501 (2015).
[26] Y. Asai, K. Sakai, K. Ishibashi, K. Takeda, and T. Yoshitake, JJAP Conf. Proc. **3**, 011504 (2015).
[27] T. Sadoh, T. Takeuchi, K. Ueda, A. Kenjo, and M. Miyao, Jpn. J. Appl. Phys. **45**, 3598 (2005).
[28] M. Shaban, H. Kondo, K. Nakashima, and T. Yoshitake, Jpn. J. Appl. Phys. **47**, 5420 (2008).
[29] Y. Sakuraba, M. Hattori, M. Oogane, Y. Ando, H. Kato, A. Sakuma, T. Miyazaki, and H. Kubota, Appl. Phys. Lett. **88**, 192508 (2006).
[30] T. Ishikawa, N. Itabashi, T. Taira, K. Matsuda, T. Uemura, and M. Yamamoto, Appl. Phys. Lett. **94**, 092503 (2009).
[31] A. Sakuma, Y. Toga, and H. Tsuchiura, J. Appl. Phys. **105**, 07C910 (2009).
[32] M. A. M. Gijs, S.K. J. Lenczowski, and J. B. Giesbers, Phys. Rev. Lett. **70**, 3343 (1993).
[33] H. Sato, Y. Aoki, Y. Kobayashi, H. Yamamoto, and T. Shinjo, J. Phys. Soc. Jpn. **62**, 431 (1993).
[34] G. Schmidt, D. Ferrand, L. W. Molenkamp, A. T. Filip, and B. J. van Wees, Phys. Rev. B **62**, R4790 (2000).
[35] E. I. Rashba, Phys. Rev. B **62**, R16267 (2000).
[36] A. Fert and H. Jaffrès, Phys. Rev. B **64**, 184420 (2001).
[37] T. Kimura, T. Sato, and Y. Otani, Phys. Rev. Lett. **100**, 066602 (2008).